Library Approach for Reliable Synthesis and Properties of DNA-Gold Nanorod Conjugates

ARTICLE *in* ANALYTICAL CHEMISTRY · JUNE 2013

Impact Factor: 5.64 · DOI: 10.1021/ac400672e · Source: PubMed

2 AUTHORS, INCLUDING:

Jae-Seung Lee
Korea University
48 PUBLICATIONS **3,281** CITATIONS

SEE PROFILE

analytical chemistry

Technical Note

pubs.acs.org/ac

Library Approach for Reliable Synthesis and Properties of DNA–Gold Nanorod Conjugates

Jang Ho Joo and Jae-Seung Lee*

Department of Materials Science and Engineering, Korea University Anam-dong, Seongbuk-gu, Seoul, 136-713, Republic of Korea

Supporting Information

ABSTRACT: We developed a library-based approach to chemically stabilize cetyltrimethylammonium bromide (CTAB)-coated gold nanorods for the synthesis of polyvalent DNA–gold nanorod conjugates (DNA–AuNRs). Eleven chemical reagents were carefully chosen to constitute an additive library and screened by UV–vis spectroscopy to evaluate their stabilizing capability for the CTAB-coated AuNRs. Interestingly, 5-bromosalicylic acid (5-BrSA) was determined to most significantly stabilize the AuNRs by inducing additional adsorption of CTAB on the rod. Importantly, these stabilized AuNRs with 5-BrSA were conjugated with thiol DNA in an exceptionally reproducible and reliable method, which led to the systematic investigation of their cooperative assembly and disassembly properties under various conditions, including different types and lengths of the DNA sequences.

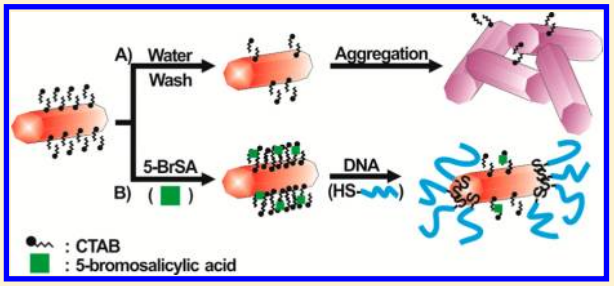

The DNA-mediated assembly of nanoparticles has been one of the fundamental paradigms in nanoscience for years.[1−5] In particular, the reversible assembly properties of the polyvalent DNA–nanoparticle conjugates ignited explosive research efforts aimed at developing new diagnostic and therapeutic applications.[6,7] Their high application potential is primarily based on the distinctive cooperative binding properties of the polyvalent DNA–nanoparticle conjugates, whose high DNA density on the particle surface plays a critical and essential role, both in theory and experiments.[8−10] Therefore, reliable, dense surface conjugation of a certain type of nanoparticles with DNA strands must be the principle key to success in utilizing such nanoparticles in different fundamental studies and applications. To date, only a few types of nanoparticles of various materials with different geometries have been demonstrated to be densely conjugated with thiol DNA at an extent sufficient to exhibit cooperative assembly properties, such as gold or silver nanospheres,[8,11] nanoplates,[12,13] nanocubes,[14] nanopolyhedra,[15] nanorods,[15−21] and even semiconductor nanospheres.[22] Among them, DNA conjugates of short one-dimensional gold nanomaterials (gold nanorods), DNA–gold nanorod conjugates (DNA–AuNRs), would be particularly attractive, because the AuNRs exhibit unique photothermal and optical properties that are highly dependent on the size and shape of the rods.[23−25] While a few demonstrations of DNA–AuNRs have been occasionally reported, they often do not provide a general synthesis strategy for DNA conjugation and a consistent set of observation of their cooperative assembly properties. Importantly, this insufficient progress is accounted for by two hypothetical reasons: (1) the weak and complicated silver–sulfur interactions of thiol DNA and AuNRs because the conjugation reaction is assisted by silver ions[15,26] and (2) the chemically stabilized cetyltrimethylammonium bromide (CTAB)-coated AuNRs' instability that is inevitably associated with their irreversible aggregate formation.[26,27] Considering the strong need for a thorough investigation of the cooperative and reversible assembly properties of DNA–AuNRs and the design of corresponding applications, the development of a general, reliable method for their synthesis would be a significant contribution.

Herein, we present a chemical method to reproducibly and reliably synthesize the polyvalent DNA–AuNRs by dramatically enhancing the stability of CTAB-coated AuNRs. Unlike the conventional ligand-exchange or layer-by-layer approaches, which have to remove or ignore the CTAB molecules on top of the nanorod surfaces prior to conjugation with other molecules, we conversely took advantage of the existing CTAB and further increased the rod surface charge by intercalating an additive chemical reagent that was selected by screening a chemical library. Subsequently, the stabilized AuNRs were efficiently conjugated with thiol DNA based on the conventional gold–sulfur chemistry,[28] without assistance of any additional protecting thiol moieties such as thiol poly(ethylene glycol).[17,29] Importantly, we systematically obtained and analyzed a series of cooperative melting properties of polyvalent DNA–AuNRs synthesized using our newly developed method under a variety of conditions.

MATERIALS AND METHODS

Materials. Cetyltrimetylammonium bromide (CTAB, 96.0%, Cat. # 52370), sodium tetrachloroaurate (III) dihydrate (99%, Cat. # 298174), sodium borohydride (98%, Cat. #

Received: March 4, 2013
Accepted: June 10, 2013
Published: June 25, 2013

   dx.doi.org/10.1021/ac400672e | Anal. Chem. 2013, 85, 6580–6586

480886), ascorbic acid (Cat. # A5960), Tween 20 (T20, Cat. # 9005-64-5), and silver nitrate (99%, Cat. # 204390) were purchased from Sigma-Aldrich (USA), and 5-bromosalicylic acid (5-BrSA, Cat. # B0895) was purchased from Tokyo Chemical Industry (Japan). The monothiol DNA sequences (**1**-$\mathbf{X_n}$: 5′ HS-X_n-ATTATCACT 3′; **2**-$\mathbf{X_n}$: 5′ HS-X_n-AGTGA-TAAT 3′; n = 6, 10, 15, 20, 25, 30, 35, and 40; X = T or A), purified by HPLC, were purchased from Genotech, Inc. (Republic of Korea).

Synthesis of Gold Nanorods (AuNRs). For the synthesis of the seeds, 5 mL of 0.2 M CTAB solution and 5 mL of 0.5 mM $NaAuCl_4$ solution were mixed in a glass vial (50 mL), to which 0.6 mL of 0.01 M fresh $NaBH_4$ solution was added and sonicated for 3 min. The mixture turned brownish-yellow, indicating the formation of gold seeds. The reaction mixture was further incubated in a water bath at 25 °C for 1 h to complete the seed formation reaction. Subsequently, the growth solution was prepared by mixing 50 mL of 0.2 M CTAB solution and 50 mL of 1 mM $NaAuCl_4$ solution in an Erlenmeyer flask (250 mL). To this mixture, 3.25 mL of 4 mM $AgNO_3$ and 0.7 mL of 78.8 mM ascorbic acid solutions were further added. Upon the addition of ascorbic acid, the color of the mixture changed from dark orange to colorless because of the reduction of Au^{3+} to Au^{+}. Finally, 0.06 mL of the seed solution was injected to the growth solution under sonication for 3 min. The mixture was covered with aluminum foil to be protected from light and incubated in a water bath at 25 °C for 1 h. The solution turned dark pink within 30 min, indicating the formation of AuNRs. The synthesized AuNRs were analyzed by transmission electron microscopy (TEM; TECNAI G^2 F30ST (FEI) operated at 300 kV), whose length and diameter were determined to be 48.4 and 13.5 nm, respectively. The AuNRs were stored in the dark at 4 °C before use.

Incubation of AuNRs with an Additive. To remove the crystallized CTAB at the bottom of the AuNR solution, it was precipitated at a lower temperature, while the supernatant containing the AuNRs was decanted and centrifuged at 6000 rpm for 30 s to completely spin down the remaining CTAB crystals. After collecting the supernatant containing the AuNRs (4 mL), it was combined with a specific additive (10 mM, 400 μL). The AuNRs were allowed to incubate with the additive at room temperature for 12 h. Finally, the AuNRs (4.4 mL) were washed two times by water (centrifugation at 10 000 rpm for 8 min, removal of the supernatant, and redispersion in 4 mL of water).

Synthesis of DNA−AuNR Conjugates. The monothiol DNA sequences (1 OD) were deprotected by a 0.10 M DTT solution (0.17 M phosphate, pH8.0), purified by a NAP-5 column, and combined with the AuNRs (500 μL). The mixed solution was buffered to 0.15 M NaCl in a phosphate buffer (0.01% T20, pH 7.4, 10 mM phosphate) and incubated for 12 h at 25 °C. To remove the unconjugated free DNA, the DNA−AuNRs were washed by centrifugation (10 000 rpm, 6 min) two times. Finally, DNA−AuNRs were redispersed in a suitable buffer solution (e.g., 0.15 M NaCl, 0.01% T20, pH 7.4, 10 mM phosphate).

RESULTS AND DISCUSSION

Our investigation began from the two aforementioned hypotheses that explain the synthesis problem of DNA−AuNRs. Considering several trustworthy examples of pure silver nanomaterial−thiol DNA conjugates,[13,14] we decided to enhance the stability of the CTAB-coated AuNRs for the synthesis of DNA−AuNRs. We first assumed that certain aromatic and aliphatic molecules that are negatively charged could intercalate into the hydrophobic region of the positively charged CTAB double layer on top of the AuNR surface[30] and, on the basis of charge considerations, would further induce a higher CTAB population and an increased surface potential. To evaluate this assumption, we carefully selected 11 organic and inorganic molecules with common negative charges, but different molecular structures and amphilicities, and built up a library of additives (from **1** to **11**; Figure 1). Importantly, the

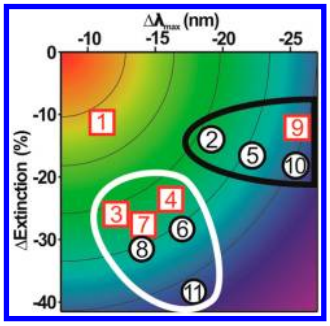

Figure 1. Eleven additives from **1** to **11** (**1**, 5-bromosalicylic acid (5-BrSA); **2**, creatine; **3**, 2,6-dihydroxybenzoic acid; **4**, salicylic acid; **5**, citric acid; **6**, boric acid; **7**, pyrazinecarboxylic acid; **8**, L-glutamic acid; **9**, benzoic acid; **10**, tartaric acid; **11**, 11-aminoundecanoic acid) distributed as a function of Δextinction and $\Delta\lambda_{MAX}$. Note that the additives containing an aromatic ring are designated with the numeric symbols in a red square, while the other additives are in a black circle.

library consists of 10 molecules containing a carboxylic group(s) in common along with the following: (1) a phenyl ring (**1**, **3**, **4**, and **9**), (2) an amine group(s) (**2**, **8**, and **11**), (3) a pyrazine ring (**7**), and (4) hydroxyl groups (**1**, **3**, **4**, **5**, and **10**). The library also includes boric acid (**6**), an inorganic acid without a carboxylic group. For the effective intercalation of these additives, the AuNR solution was first incubated with each additive for 12 h at 25 °C. The color of the mixtures remained the same after incubation, indicating that the AuNRs with additives did not exhibit any noticeable difference in stability under mild conditions. To select the most effective additive for the stabilization of the AuNRs, the mixtures were further evaluated under harsher conditions by repeated centrifugation of the AuNRs, removal of the supernatant, and redispersion in a desired solution. This three-step procedure, where AuNRs are closely packed by the centrifugal force and redispersed without unexpected impurities, is commonly considered as "wash." Specifically, from the viewpoint of colloidal chemistry, the centrifugation dramatically reduces the interparticle distances and, thus, maximizes the effect of van der Waals force between the AuNRs to increase their attractive interactions.[31] While the stable AuNRs with strong electrostatic repulsion can survive and are readily dispersed again during this procedure, the unstable AuNRs are supposed to aggregate irreversibly, leading to changes in extinction and λ_{MAX} (the wavelength where the maximum extinction takes place). In fact, the extinction and λ_{MAX} of the UV−vis spectra of the plasmonic nanomaterials are known as the most efficient indicators of their stable dispersion in solution.[32−35] Therefore, the stability of the AuNRs after a wash with water was observed by monitoring their UV−vis spectra. The decrease in the maximum extinction ($\Delta\varepsilon_{MAX}$) and the shift of the λ_{MAX} before and after the wash of the AuNRs were taken as quantitative

dx.doi.org/10.1021/ac400672e | Anal. Chem. 2013, 85, 6580−6586

measurements (see Supporting Information for the resultant UV−vis spectra, Figure S-1). The effect of each additive on $\Delta\varepsilon_{MAX}$ and $\Delta\lambda_{MAX}$ of the AuNRs is demonstrated in Figure 1. Obviously, **1** (5-bromosalicylic acid; 5-BrSA) turned out to induce the least amount of change both in $\Delta\varepsilon_{MAX}$ (∼−10%) and $\Delta\lambda_{MAX}$ (∼−10 nm), indicative of the greatest potential of 5-BrSA to stabilize the AuNRs. The other additives formed two main categories: (1) additives leading to a stronger decrease in $\Delta\varepsilon_{MAX}$ (**3**, **4**, **6**, **7**, **8**, and **11** in the white boundary in Figure 1; $|\Delta\lambda_{MAX}| < 20$ nm; $|\Delta\varepsilon_{MAX}| > 20\%$) and (2) those reducing $\Delta\lambda_{MAX}$ more strongly (**2**, **5**, **9**, and **10** in the black boundary in Figure 1; $|\Delta\lambda_{MAX}| > 20$ nm; $|\Delta\varepsilon_{MAX}| < 20\%$). Interestingly, from the perspective of the molecular structure, we noticed that the additives containing an aromatic ring tended to induce a larger shift in $\Delta\varepsilon_{MAX}$ (**3**, **4**, and **7**) than in $\Delta\lambda_{MAX}$ (**9**), while the nonaromatic additives equally affect both $\Delta\varepsilon_{MAX}$ (**8**, **6**, and **11**) and $\Delta\lambda_{MAX}$ (**2**, **5**, and **10**).

We further quantitatively explored the stabilizing effect of 5-BrSA on the AuNRs under harsher conditions including repeated washes. For comparison, we prepared three batches of AuNRs: the AuNRs repeatedly washed with solutions containing (1) an excess of CTAB ($AuNR_{(CTAB)}$s; [CTAB] = 0.5 mM), (2) no CTAB but water only ($AuNR_{(Water)}$s), and (3) no CTAB but water only, which were, however, incubated with 5-BrSA for 12 h prior to the wash ($AuNR_{(5BrSA)}$s). The stability of the $AuNR_{(CTAB)}$s was observed by UV−vis spectroscopy and quantitatively evaluated (Figure 2). After the first centrifugation, the maximum extinction at λ_{MAX} (∼724 nm) slightly decreased, which was probably because of the irreversible aggregation of a few innately unstable AuNRs by the centrifugal force (Figure 2A). After repeated washes up to three times, however, the changes in both the ε_{MAX} and λ_{MAX} of the

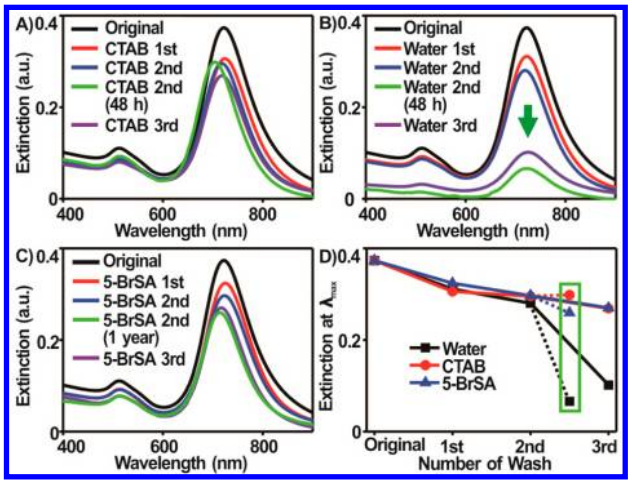

Figure 2. UV−vis spectra of the AuNRs repeatedly washed with (A) CTAB-containing solution ($AuNR_{(CTAB)}$), (B) pure water ($AuNR_{(Water)}$), and (C) pure water after the incubation with 5-BrSA for 12 h ($AuNR_{(5BrSA)}$) before the wash. Note that only the $AuNR_{(Water)}$s exhibit a dramatic decrease in extinction after the second wash, indicative of the irreversible AuNR aggregation. (D) The extinction at λ_{MAX} of AuNRs washed with different washing solutions once, twice, and thrice. The extinctions at λ_{MAX} of AuNRs with a time lapse (48 h or 1 year) after the second wash are designated in a green box between the second and the third washes. Note that the AuNRs washed three times with each solution (CTAB third, Water third, and 5-BrSA third) were obtained from the AuNRs after the second wash without any incubation time (CTAB second, Water second, and 5-BrSA second).

$AuNR_{(CTAB)}$s were almost negligible and even remained constant for at least 48 h after the second wash. The λ_{MAX} of the $AuNR_{(CTAB)}$s after the second wash exhibited a slight blue-shift.[36,37] This observation clearly shows the substantial stability of AuNRs in the presence of excess CTAB. As reported previously, however, these redispersed stable AuNRs in 0.5 mM CTAB solution immediately aggregated and precipitated upon the addition of thiol DNA (see Supporting Information, Figure S-2).[15] In fact, not only AuNRs but also spherical silver nanoparticles capped with positively charged ligands such as CTAB were reported to irreversibly aggregate upon the addition of thiol DNA, which by analogy, supports our observation.[38]

Considering that an excess of CTAB is a problem because of formation of aggregates with negatively charged DNA and, consequently, with the AuNRs,[39] we took advantage of the wash process to remove the excess CTAB prior to conjugation, by repeatedly washing the particles with water devoid of CTAB. In fact, this precedent wash process for the removal of the excess ligand is generally conducted to ensure DNA conjugation of other nanoparticles.[13,14] Once washed, however, the $AuNR_{(Water)}$s would lose the protecting CTAB because of desorption of CTAB from the rod surface, which could risk their stability.[40,41] To verify this theory, we observed the UV−vis spectra of the AuNRs after repeated washes with pure water ($AuNR_{(Water)}$s; Figure 2B). As expected, the ε_{MAX} significantly decreased after the third wash owing to the release of CTAB molecules from the $AuNR_{(Water)}$ surface and consequent aggregation of the destabilized $AuNR_{(Water)}$s. Already after the second wash, the ε_{MAX} decreased to ∼20% of the initial value within 48 h, indicating a gradual desorption of CTAB with the lapse of time. For the DNA conjugation of the AuNRs, the excess CTAB was washed out twice, and the AuNRs were immediately combined with thiol DNA, which however, could result in the maintained optical properties of the AuNRs with a probability of only ∼30%.[41,42] This result illustrates the dilemma: an excess of CTAB stabilizes the AuNRs but fails in DNA conjugation; the removal of excess CTAB hardly stabilizes the AuNRs, but it still does not reliably ensure their reproducible DNA conjugation.

We finally investigated the stabilizing effect of 5-BrSA with respect to the AuNRs ($AuNR_{(5BrSA)}$s). After incubation with 5-BrSA for 12 h, the $AuNR_{(5BrSA)}$s exhibited an unusually increased stability, evidenced by the almost unchanged UV−vis spectra after repeated washes, up to three times, with water containing neither CTAB nor 5-BrSA (Figure 2C). Very importantly, the time-dependent release of CTAB from the AuNR surface and consequent destabilization of the AuNRs were not observed for up to one year after the second wash. The wash-dependent changes in extinction at λ_{MAX} of each type of AuNRs ($AuNR_{(CTAB)}$s, $AuNR_{(Water)}$s, and $AuNR_{(5BrSA)}$s) are shown in Figure 2D, where both $AuNR_{(CTAB)}$s (red circles) and $AuNR_{(5BrSA)}$s (blue triangles) exhibit almost the same stability up to the third wash or for an extended time after the second wash (green box). In the case of $AuNR_{(Water)}$s (black squares), however, the extinction decreases to <25% of the original value after the third wash or within 48 h after the second wash. These spectroscopic analyses of the AuNRs' stability-dependent optical properties under various conditions evidently demonstrate the straightforward and convincing contribution of 5-BrSA to the stabilization of AuNRs.

The substantial contrast of the stability changes between $AuNR_{(5BrSA)}$s and $AuNR_{(Water)}$s after repeated washes was

dx.doi.org/10.1021/ac400672e | Anal. Chem. 2013, 85, 6580−6586

further examined by measuring the zeta potential (ζ) of these AuNRs (Figure 3). The ζ of as-synthesized AuNRs in the presence of excess CTAB was 52.88 mV, which decreased to 36.80 mV after a wash with water ($AuNR_{(Water)}$) owing to the desorption of the positively charged CTAB molecules. On the other hand, however, the ζ of the as-synthesized AuNR incubated with 5-BrSA for 12 h increased up to 73.41 mV, indicating an additional adsorption of CTAB on the AuNRs. The ζ of $AuNR_{(5BrSA)}$s after a wash with water still reached at 52.53 mV, which is far higher than that of the washed $AuNR_{(Water)}$s (36.80 mV). The consistently higher ζ of $AuNR_{(5BrSA)}$s compared to that of $AuNR_{(Water)}$s, before or after the wash, or even after the DNA conjugation (vide infra), not only explains the enhanced stability of $AuNR_{(5BrSA)}$s owing to the increased CTAB but also suggests a method to understand the fundamental role that 5-BrSA plays (Scheme 1). The increased ζ of $AuNR_{(5BrSA)}$s is primarily attributed to two important properties of 5-BrSA: (1) intercalation of 5-BrSA into the CTAB double layer on the AuNRs[30,43,44] and (2) negative charge of the carboxyl group, which attracts positively charged CTAB molecules. Under our experimental conditions, most of the 5-BrSA molecules are expected to be deprotonated (>99%) because of the lower pK_a of 5-BrSA (pK_a = 2.6 at 25 °C)[45] and higher pH of the mixture medium containing the as-synthesized AuNRs (after the solid CTAB is removed) incubated with 5-BrSA (pH = ~6). Meanwhile, the deprotonated carboxyl group of the intercalated 5-BrSA is exposed at the outer surface of the CTAB layer,[30,46] whose negative charge attracts more CTAB molecules onto the AuNR surface (Scheme 1B). On the other hand, $AuNR_{(Water)}$s do not involve such a protecting mechanism and would merely lose their surface CTAB, thus leading to the observed irreversible nanorod aggregation (Scheme 1A).

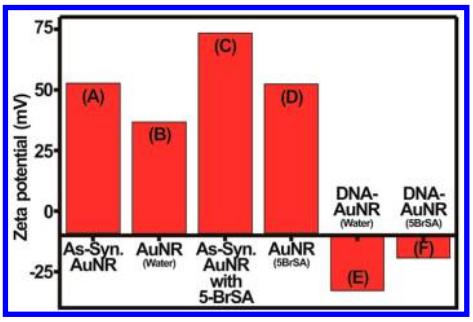

Figure 3. Zeta potential measurement of the (A) as-synthesized AuNRs, (B) washed AuNRs with water, (C) as-synthesized AuNRs incubated with 5-BrSA, (D) AuNRs incubated with 5-BrSA and washed with water, (E) AuNRs that were washed with water and conjugated with DNA, and (F) AuNRs incubated with 5-BrSA, washed with water, and conjugated with DNA.

Scheme 1. Scheme Depicting (A) the Desorption of CTAB from the AuNR Surface by the Wash with Pure Water, Followed by an Irreversible Aggregation of the AuNRs, and (B) the Intercalation of 5-BrSA Followed by the Wash with Pure Water[a]

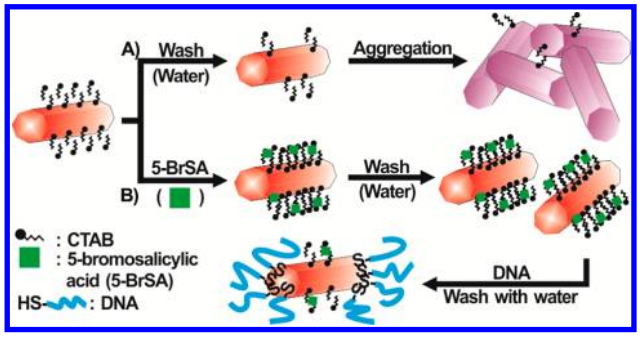

[a]The intercalation of 5-BrSA induces an increased adsorption of CTAB on the AuNR, which in turn, leads to an increased surface potential and thus to an enhanced stability of the AuNRs. The stabilized AuNRs were further conjugated with thiol DNA and washed with water to eliminate the excess DNA. The cross-section of the rods is described to be octagonal based on previous literature.[66].

After probing the role and the effect of 5-BrSA on the enhanced stability of CTAB-coated AuNRs, we further investigated the synthesis and properties of DNA–AuNRs using electron microscopy and UV–vis spectroscopy. We first observed the morphology of the AuNRs before and after 5-BrSA incubation, as well as after DNA conjugation, using transmission electron microscopy (TEM). The as-synthesized AuNRs exhibited typical rod-like shapes with a length of 48.4 nm and a diameter of 13.5 nm on average (Figure 4A), which did not change after overnight incubation with 5-BrSA and subsequent DNA conjugation (Figure 4B,C, respectively). The optical properties of the AuNRs were sequentially obtained using UV–vis spectroscopy (Figure 4D). The as-synthesized AuNRs exhibited a narrow plasmon band at ~730 nm (black), whose λ_{MAX} and ε_{MAX} did not exhibit any noticeable change after overnight incubation with 5-BrSA (red) and subsequent DNA conjugation (blue), indicating a significantly enhanced stability of the $AuNR_{(5BrSA)}$s, sufficient to overcome the loss of the protecting CTAB during DNA conjugation. To confirm that the thiol DNA strands were functionally conjugated with the AuNRs, we further prepared AuNRs conjugated with the complementary DNA sequences and combined the two complementary types of DNA–AuNRs for their hybridization.

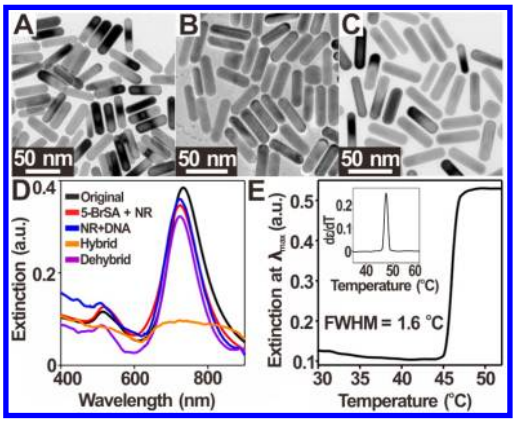

Figure 4. Transmission electron microscopy (TEM) images of AuNRs: (A) as-synthesized, (B) incubated with 5-BrSA, and (C) conjugated with thiol DNA. (D) UV–vis spectra of different AuNRs: as-synthesized, incubated with 5-BrSA, conjugated with DNA, DNA conjugated and hybridized with complementary DNA–AuNRs, and dehybridized. Note that $\Delta\lambda_{MAX}$ of the as-synthesized AuNRs and the finally dehybridized DNA–AuNRs is less than 7 nm. (E) A melting transition of hybridized DNA–AuNRs and its first derivative (inset). Note that the full width at half-maximum (fwhm) of the transition curve is only 1.6 °C, typically indicative of densely loaded DNA strands and consequent cooperative binding properties.

dx.doi.org/10.1021/ac400672e | Anal. Chem. 2013, 85, 6580–6586

After several hours, the spectrum of the hybridized DNA–AuNRs exhibited a much broader curve (orange), typically observed for other hybridized DNA–plasmonic nanoparticle conjugates.[8,11,13,14] Importantly, on heating, the plasmonic band recovered almost to its original form in terms of λ_{MAX} and ε_{MAX} (purple), strongly indicative of a functional DNA conjugation with the AuNRs and their reversible interconnect formation with complementary ones. The melting profile of the hybridized DNA–AuNRs was observed by monitoring ε_{MAX} at 730 nm as a function of temperature, which exhibits an extremely sharp melting transition whose full width at half-maximum (fwhm) was only 1.6 °C (Figure 4E). Incredibly, we were also able to conjugate the thiol DNA with the one-year-old AuNRs after the incubation with 5-BrSA and obtained the same, sharp melting transition (see Supporting Information, Figure S-3). These sharp melting transitions are a convincing evidence of the high DNA density on the AuNR surface, essential for their potential diagnostic and therapeutic applications.[8,47,48]

Whether the DNA–AuNRs synthesized using 5-BrSA exhibit similar cooperative melting properties as their analogues, however, still remains to be elucidated, particularly if their anisotropic morphologies are taken into consideration. To validate their cooperative properties, we systematically investigated the melting profiles of DNA–AuNRs under various conditions, including different salt concentrations, and spacer type/length of the DNA sequences. Two complementary DNA–AuNRs were combined for hybridization at various NaCl concentrations, ([NaCl]s) ranging from 0.1 to 0.6 M, and monitored at 730 nm while heated up to 65 °C for their dehybridization (Figure 5A, inset). The obtained melting

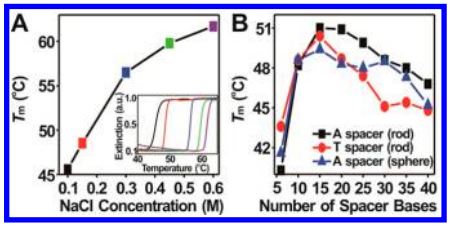

Figure 5. (A) A plot of the melting temperatures (T_ms) as a function of the NaCl concentration employed during DNA–AuNR hybridization and their corresponding melting transitions (inset). Note that the color of the melting transitions in the inset matches that of the squares representing the corresponding NaCl concentration. (B) A plot of T_ms as a function of the spacer length of the hybridized DNA–AuNRs containing either polyadenine (A_n) or polythymine (T_n) spacers and hybridized DNA–spherical gold nanoparticle conjugates containing the polyadenine (A_n) spacer.

temperatures (T_ms)[49] were plotted as a function of [NaCl] (Figure 5A), exhibiting a strong correlation as reported for other DNA–plasmonic nanoparticle conjugates. Interestingly, in contrast to DNA-conjugated nanoplates,[13] no stepwise increase in the melting curves was observed for the presently investigated DNA–AuNRs. This observation clearly indicates that the DNA strands are immobilized preferentially, or even exclusively, at and near the end of the rods, as proposed for other surface-modification of AuNRs,[50−54] and therefore, that there exists only a single type of "end-to-end" hybridization.

In addition, we investigated the assembly properties of the hybridized DNA–AuNRs with different "spacers" that are composed of various numbers of monomeric nucleotides (polythymine (T_n) or polyadenine (A_n)) between the thiol group and the sequence portion associated with the hybridization, by obtaining their melting transitions (Figure 5B). Importantly, compared to previous studies on spacers which explored up to n = 15 for spherical nanoparticles[8] and up to n = 30 for cubic ones,[14] we significantly extended the spacer length up to n = 40 in this work. At n = 6, the T_m of the DNA–AuNRs with T_6 (43.6 °C) was higher than the one with A_6 spacers (40.3 °C), which can be attributed to the greater adsorption of adenine on the gold surface than thymine, as observed for DNA–spherical gold nanoparticles conjugates.[55,56] As n increased to 15, the T_m of the DNA–AuNRs gradually increased up to ∼51 °C and subsequently decreased from n = 20 to n = 40. In fact, the initial increase and subsequent decrease of the T_m of the DNA–AuNRs as a function of spacer length was previously reported for the silver cubic nanostructures by our group,[14] where the flat surface structure was proposed to play a crucial role. For example, the larger curvature of the DNA–spherical nanoparticle conjugates allows the DNA sequences that are far from the conjugate–conjugate contact point to obtain greater accessibility when they have longer spacers. On the other hand, the flat surface of the AuNRs would always provide the same accessibility to the DNA strands when they hybridize with the complementary sequences. Under such conditions, the charge-induced repulsion dominates the DNA–AuNR interactions, resulting in a decrease in T_m of the DNA–AuNRs containing longer spacers. Although the end of the AuNRs is not completely flat, their curvature is still expected to be much smaller than that of spherical nanoparticles, which explains the results obtained in Figure 5B.[57] For comparison, we measured the melting transitions of DNA–spherical gold nanoparticle conjugates, which exhibit a similar tendency up to n = 15, but later show a much gentler down slope up to n = 30. This almost flat portion of the curve between n = 15 and n = 30 is the result of a compromise between an increase in T_m induced by the sphere's curvature and decrease in T_m induced by repulsive charge interactions.[8] Eventually, however, the repulsive interactions of the DNA–AuNRs may become dominant and then lead to the dramatic decrease in T_m down to 45.2 °C (Figure 5B). Consequently, the flat portion of the T_m curve of the DNA–spherical gold nanoparticles resulted in a smaller difference between the highest and lowest T_ms (4.1 °C; $n \geq 15$) compared to the DNA–AuNRs with A_n and T_n spacers (4.3 and 5.6 °C, respectively; $n \geq 15$). The collection of these data reveals the significant effect of slight structural changes on the chemical and physical properties of nanomaterials, which is demonstrated only by DNA conjugation of AuNRs described in this work.

■ CONCLUSIONS

In this Technical Note, we demonstrate the highly reproducible, reliable, and facile DNA conjugation method for CTAB-coated AuNRs. This method is designed according to a two-step analytical approach: (1) screening of the 11 chemical additives containing various functionalities for the stabilization of AuNRs and (2) remarkably enhancing the stability of CTAB-coated AuNRs prior to DNA conjugation, using 5-BrSA that is selected from the chemical library. The melting properties of hybridized DNA–AuNRs are thoroughly analyzed as a function of the lengths and base types of the DNA spacers and further compared with those of conventional DNA–spherical nanoparticles conjugates. The development of the reliable, facile synthetic method for the DNA–AuNRs in this work would lead

dx.doi.org/10.1021/ac400672e | Anal. Chem. 2013, 85, 6580−6586

to an explosive extension of the various diagnostic and therapeutic applications of DNA–AuNRs.[17,29,58−63] Importantly, this library-based chemical stabilization would be easily generalized for the conjugation of thiol DNA with other CTAB-coated nanomaterials whose stability during the conjugation procedure needs to be significantly and carefully considered.[38,64,65]

■ ASSOCIATED CONTENT

Supporting Information

Experimental procedures and additional UV−vis spectra and melting profiles. This material is available free of charge via the Internet at http://pubs.acs.org.

■ AUTHOR INFORMATION

Corresponding Author

*E-mail: JSLEE79@korea.ac.kr. Fax: +82-2-928-3584.

Notes

The authors declare no competing financial interest.

■ ACKNOWLEDGMENTS

This work was supported by Basic Science Research Program through the National Research Foundation of Korea (NRF) funded by the Ministry of Education, Science and Technology (Grant No. 2012R1A1A2A10042814 and NRF-2013-Global Ph.D. Fellowship Program). Ms. Yun Kyong Sung (Sam Bo Scientific Co., Ltd) is acknowledged for her help with the zeta potential measurement.

■ REFERENCES

(1) Mirkin, C. A.; Letsinger, R. L.; Mucic, R. C.; Storhoff, J. J. *Nature* **1996**, *382*, 607−609.
(2) Nykypanchuk, D.; Maye, M. M.; van der Lelie, D.; Gang, O. *Nature* **2008**, *451*, 549−552.
(3) Alivisatos, A. P.; Johnsson, K. P.; Peng, X.; Wilson, T. E.; Loweth, C. J.; Bruchez, M. P.; Schultz, P. G. *Nature* **1996**, *382*, 609−611.
(4) Wang, H.; Yang, R.; Yang, L.; Tan, W. *ACS Nano* **2009**, *3*, 2451−2460.
(5) Tan, S. J.; Campolongo, M. J.; Luo, D.; Cheng, W. L. *Nat. Nanotechnol.* **2011**, *6*, 268−276.
(6) Huang, C.-C.; Huang, Y.-F.; Cao, Z.; Tan, W.; Chang, H.-T. *Anal. Chem.* **2005**, *77*, 5735−5741.
(7) Prow, T.; Smith, J. N.; Grebe, R.; Salazar, J. H.; Wang, N.; Kotov, N.; Lutty, G.; Leary, J. *Mol. Vision* **2006**, *12*, 606−615.
(8) Jin, R.; Wu, G.; Li, Z.; Mirkin, C. A.; Schatz, G. C. *J. Am. Chem. Soc.* **2003**, *125*, 1643−1654.
(9) Lytton-Jean, A. K. R.; Mirkin, C. A. *J. Am. Chem. Soc.* **2005**, *127*, 12754−12755.
(10) Gibbs-Davis, J. M.; Schatz, G. C.; Nguyen, S. T. *J. Am. Chem. Soc.* **2007**, *129*, 15535−15540.
(11) Dougan, J. A.; Karisson, C.; Smith, W. E.; Graham, D. *Nucleic Acids Res.* **2007**, *35*, 3668−3675.
(12) Millstone, J. E.; Georganopoulou, D. G.; Xu, X.; Wei, W.; Li, S.; Mirkin, C. A. *Small* **2008**, *4*, 2176−2180.
(13) Kim, J. Y.; Lee, J.-S. *Chem. Mater.* **2010**, *22*, 6684−6691.
(14) Park, H. G.; Joo, J. H.; Kim, H. G.; Lee, J. S. *J. Phys. Chem. C* **2012**, *116*, 2278−2284.
(15) Jones, M. R.; Macfarlane, R. J.; Lee, B.; Zhang, J.; Young, K. L.; Senesi, A. J.; Mirkin, C. A. *Nat. Mater.* **2010**, *9*, 913−917.
(16) Dujardin, E.; Hsin, L.-B.; Wang, C. R. C.; Mann, S. *Chem. Commun.* **2001**, 1264−1265.
(17) Yasun, E.; Gulbakan, B.; Ocsoy, I.; Yuan, Q.; Shukoor, M. I.; Li, C. M.; Tan, W. H. *Anal. Chem.* **2012**, *84*, 6008−6015.
(18) Chen, C. C.; Lin, Y. P.; Wang, C. W.; Tzeng, H. C.; Wu, C. H.; Chen, Y. C.; Chen, C. P.; Chen, L. C.; Wu, Y. C. *J. Am. Chem. Soc.* **2006**, *128*, 3709−3715.
(19) Pal, S.; Deng, Z. T.; Wang, H. N.; Zou, S. L.; Liu, Y.; Yan, H. *J. Am. Chem. Soc.* **2011**, *133*, 17606−17609.
(20) Shi, D. W.; Song, C.; Jiang, Q.; Wang, Z. G.; Ding, B. Q. *Chem. Commun.* **2013**, *49*, 2533−2535.
(21) Wijaya, A.; Hamad-Schifferli, K. *Langmuir* **2008**, *24*, 9966−9969.
(22) Mitchell, G. P.; Mirkin, C. A.; Letsinger, R. L. *J. Am. Chem. Soc.* **1999**, *121*, 8122−8123.
(23) Jana, N. R.; Gearheart, L.; Murphy, C. J. *Adv. Mater.* **2001**, *13*, 1389−1393.
(24) Nikoobakht, B.; El-Sayed, M. A. *Chem. Mater.* **2003**, *15*, 1957−1962.
(25) Alkilany, A. M.; Thompson, L. B.; Boulos, S. P.; Sisco, P. N.; Murphy, C. J. *Adv. Drug Delivery Rev.* **2012**, *64*, 190−199.
(26) Wang, Y. S.; Aili, D.; Selegard, R.; Tay, Y.; Baltzer, L.; Zhang, H.; Liedberg, B. *J. Mater. Chem.* **2012**, *22*, 20368−20373.
(27) Vigderman, L.; Khanal, B. P.; Zubarev, E. R. *Adv. Mater.* **2012**, *24*, 4811−4841.
(28) Häkkinen, H. *Nat. Chem.* **2012**, *4*, 443−455.
(29) Kinnear, C.; Dietsch, H.; Clift, M. J. D.; Endes, C.; Rutishauser, B. R.; Petri-Fink, A. *Angew. Chem., Int. Ed.* **2013**, *52*, 1934−1938.
(30) Ye, X. C.; Jin, L. H.; Caglayan, H.; Chen, J.; Xing, G. Z.; Zheng, C.; Vicky, D. N.; Kang, Y. J.; Engheta, N.; Kagan, C. R.; Murray, C. B. *ACS Nano* **2012**, *6*, 2804−2817.
(31) Schmid, G. *Nanoparticles: From Theory to Application*; John Wiley & Sons: Weinheim, 2006.
(32) Willets, K. A.; Van Duyne, R. P. *Annu. Rev. Phys. Chem.* **2007**, *58*, 267−297.
(33) Mulvaney, P. *Langmuir* **1996**, *12*, 788−800.
(34) Lu, X. M.; Rycenga, M.; Skrabalak, S. E.; Wiley, B.; Xia, Y. N. *Annu. Rev. Phys. Chem.* **2009**, *60*, 167−192.
(35) Ghosh, S. K.; Pal, T. *Chem. Rev.* **2007**, *107*, 4797−4862.
(36) Damm, C.; Segets, D.; Yang, G. A.; Vieweg, B. F.; Spiecker, E.; Peukert, W. *Small* **2011**, *7*, 147−156.
(37) Iqbal, M.; Tae, G. *J. Nanosci. Nanotechnol.* **2006**, *6*, 3355−3359.
(38) van Lierop, D.; Krpetic, Z.; Guerrini, L.; Larmour, I. A.; Dougan, J. A.; Faulds, K.; Graham, D. *Chem. Commun.* **2012**, *48*, 8192−8194.
(39) Grueso, E.; Cerrillos, C.; Hidalgo, J.; Lopez-Cornejo, P. *Langmuir* **2012**, *28*, 10968−10979.
(40) Gomez-Grana, S.; Hubert, F.; Testard, F.; Guerrero-Martinez, A.; Grillo, I.; Liz-Marzan, L. M.; Spalla, O. *Langmuir* **2012**, *28*, 1453−1459.
(41) Takahashi, H.; Niidome, Y.; Niidome, T.; Kaneko, K.; Kawasaki, H.; Yamada, S. *Langmuir* **2006**, *22*, 2−5.
(42) We prepared 50 independent batches of the DNA−AuNRs using this procedure, and only 17 batches of the DNA−AuNRs survived after the DNA conjugation.
(43) Lin, Z.; Cai, J. J.; Scriven, L. E.; Davis, H. T. *J. Phys. Chem.* **1994**, *98*, 5984−5993.
(44) Hassan, P. A.; Yakhmi, J. V. *Langmuir* **2000**, *16*, 7187−7191.
(45) Bray, L. G.; Dippy, J. F. J.; Hughes, S. R. C.; Laxton, L. W. *J. Chem. Soc.* **1957**, 2405−2408.
(46) Rao, U. R. K.; Manohar, C.; Valaulikar, B. S.; Iyer, R. M. *J. Phys. Chem.* **1987**, *91*, 3286−3291.
(47) Kiang, C.-H. *Phys. A* **2003**, *321*, 164−169.
(48) Rosi, N. L.; Giljohann, D. A.; Thaxton, C. S.; Lytton-Jean, A. K. R.; Han, M. S.; Mirkin, C. A. *Science* **2006**, *312*, 1027−1030.
(49) A melting temperature is typically obtained from the temperature where the maximum of the first derivative of the melting transition occurs.
(50) Petukhova, A.; Greener, J.; Liu, K.; Nykypanchuk, D.; Nicolay, R.; Matyjaszewski, K.; Kumacheva, E. *Small* **2012**, *8*, 731−737.
(51) Caswell, K. K.; Wilson, J. N.; Bunz, U. H. F.; Murphy, C. J. *J. Am. Chem. Soc.* **2003**, *125*, 13914−13915.
(52) Chang, J. Y.; Wu, H. M.; Chen, H.; Ling, Y. C.; Tan, W. H. *Chem. Commun.* **2005**, 1092−1094.

(53) Sudeep, P. K.; Joseph, S. T. S.; Thomas, K. G. *J. Am. Chem. Soc.* **2005**, *127*, 6516−6517.
(54) Wang, Y.; DePrince, A. E.; Gray, S. K.; Lin, X. M.; Pelton, M. *J. Phys. Chem. Lett.* **2010**, *1*, 2692−2698.
(55) Storhofff, J. J.; Elghanian, R.; Mirkin, C. A.; Letsinger, R. L. *Langmuir* **2002**, *18*, 6666−6670.
(56) Hurst, S. J.; Lytton-Jean, A. K. R.; Mirkin, C. A. *Anal. Chem.* **2006**, *78*, 8313−8318.
(57) Goris, B.; Bals, S.; Van den Broek, W.; Carbo-Argibay, E.; Gomez-Grana, S.; Liz-Marzan, L. M.; Van Tendeloo, G. *Nat. Mater.* **2012**, *11*, 930−935.
(58) Huang, H.; Chen, S.; Liu, F.; Zhao, Q.; Liao, B.; Yi, S.; Zeng, Y. *Anal. Chem.* **2013**, *85*, 2313−2319.
(59) Xu, L. G.; Kuang, H.; Wang, L. B.; Xu, C. L. *J. Mater. Chem.* **2011**, *21*, 16759−16782.
(60) Zhu, Y. Y.; Xu, L. G.; Ma, W.; Xu, Z.; Kuang, H.; Wang, L. B.; Xu, C. L. *Chem. Commun.* **2012**, *48*, 11889−11891.
(61) Wang, L.; Zhu, Y.; Xu, L.; Chen, W.; Kuang, H.; Liu, L.; Agarwal, A.; Xu, C.; Kotov, N. A. *Angew. Chem., Int. Ed.* **2010**, *49*, 5472−5475.
(62) Eghtedari, M.; Oraevsky, A.; Copland, J. A.; Kotov, N. A.; Conjusteau, A.; Motamedi, M. *Nano Lett.* **2007**, *7*, 1914−1918.
(63) Podsiadlo, P.; Sinani, V. A.; Bahng, J. H.; Kam, N. W. S.; Lee, J.; Kotov, N. A. *Langmuir* **2008**, *24*, 568−574.
(64) Baruah, B.; Craighead, C.; Abolarin, C. *Langmuir* **2012**, *28*, 15168−15176.
(65) Jana, N. R.; Gearheart, L.; Murphy, C. J. *Langmuir* **2001**, *17*, 6782−6786.
(66) Smith, D. K.; Miller, N. R.; Korgel, B. A. *Langmuir* **2009**, *25*, 9518−9524.